Published in final edited form as:
Neurobiol Dis. 2013 January ; 0: 13–21. doi:10.1016/j.nbd.2012.08.016.

A screen for inducers of p21 $^{waf1/cip1}$ identifies HIF prolyl hydroxylase inhibitors as neuroprotective agents with antitumor properties

Thong C. Ma, PhD[a,b,*], **Brett Langley, PhD**[a,b], **Brian Ko, BS**[a,b], **Na Wei, MS**[d], **Irina G. Gazaryan, PhD**[a,b], **Neela Zareen, BS**[c], **Darrell J. Yamashiro, MD PhD**[d], **Dianna E. Willis, PhD**[a,b], and **Rajiv R. Ratan, MD PhD**[a,b,*]

[a]Burke-Cornell Medical Research Institute 785 Mamaroneck Avenue, White Plains, NY 10605, USA

[b]Department of Neurology and Neuroscience, Weill Medical College of Cornell University, 525 East 68th Street, New York, NY 10065, USA

[c]Department of Pathology, Columbia University College of Physicians and Surgeons, 630 West 168th Street, New York, NY, 10032, USA

[d]Department of Pediatrics, Pathology, and Cell Biology, Columbia University College of Physicians and Surgeons, 161 Fort Washington Avenue, New York, NY 10032, USA

Abstract

Preventing neuronal death is a priority for treating neurological diseases. However, therapies that inhibit pathological neuron loss could promote tumorigenesis by preventing the physiological death of cancerous cells. To avert this, we targeted the transcriptional upregulation of p21$^{waf1/cip1}$ (p21), an endogenous tumor suppressor with neuroprotective and pro-regenerative activity. We identified potential p21 indcuers by screening a FDA-approved drug and natural product small molecule library against hippocampal HT22 cells stably expressing a luciferase reporter driven by the proximal 60 bp of the p21 promoter, and tested them for neuroprotection from glutathione depletion mediated oxidative stress, and cytotoxicity to cancer cell lines (DLD-1, Neuro-2A, SH-SY5Y, NGP, CHLA15, CHP212, and SK-N-SH) *in vitro*. Of the p21 inducers identified, only ciclopirox, a hypoxia-inducible factor prolyl-4-hydroxylase (HIF-PHD) inhibitor, simultaneously protected neurons from glutathione depletion and decreased cancer cell proliferation at concentrations that were not basally toxic to neurons. We found that other structurally distinct HIF-PHD inhibitors (desferrioxamine, 3,4-dihydroxybenzoate, and dimethyloxalyl glycine) also protected neurons at concentrations that killed cancer cells. HIF-PHD inhibitors stabilize HIF transcription factors, mediating genetic adaptation to hypoxia. While augmenting HIF stability is

* Corresponding Authors: Rajiv R. Ratan M.D., Ph.D. or Thong C. Ma, Ph.D. Burke-Cornell Medical Research Institute 785 Mamaroneck Avenue, White Plains, NY 10605 Tel: 914-597-2851 Fax: 914-597-2225 rratan@burke.org or tma@burke.org.

believed to promote tumorigenesis, we found that chronic HIF-PHD inhibition killed cancer cells, suggesting a protumorigenic role for these enzymes. Moreover, our findings suggest that PHD inhibitors can be used to treat neurological disease without significant concern for cell-autonomous tumor promotion.

Keywords

p21; neuroprotection; antitumor; prolyl hydroxylase inhibitors; neuronal oxidative stress

Introduction

Therapeutics aimed at preserving neurons, preventing secondary apoptosis, and promoting regeneration in chronic neurodegenerative conditions will require long-term administration. As these agents may directly modulate cell survival or cell death pathways, they pose the risk of increasing tumor formation and carcinogenesis. To overcome this potential complication, we have conducted an unbiased screen for small molecules that upregulate the transcription of $p21^{waf1/cip1}$ (p21 hereafter), a target which has been associated with neuronal protection and suppression of tumor growth.

p21 is a member of the Cip/Kip family of cyclin-dependent kinase (Cdk) inhibitors that negatively modulates the cell cycle by binding and inhibiting cyclin-Cdk complexes or blocking DNA synthesis by binding the proliferating cell nuclear antigen. Induction or ectopic expression of p21 can inhibit mitotic cell proliferation and cause the terminal differentiation of some cell types. As a transcriptional target of p53, p21 mediates cell cycle arrest following DNA damage. As such, p21 is an important regulator of proliferation during development, differentiation, and tumorigenesis (Gartel and Radhakrishnan, 2005). Paradoxically, p21 can suppress apoptosis by stalling the cell cycle to allow DNA repair before critical transitions, and, independent of Cdk inhibition, can directly block proapoptotic effectors in the cytosol such as apoptosis signal-regulating kinase 1 (Gartel and Tyner, 2002).

p21 has been reported to prevent apoptosis in cell cycle-dependent and -independent models of neuron death. Nerve growth factor (NGF) deprivation of sympathetic neurons causes apoptosis secondary to cell cycle reentry, which can be blocked by overexpressing p21 (Park et al., 1997). As markers of aberrant cell cycle activation are expressed by the vulnerable neurons in many neurological diseases (i.e., stroke, spinal cord injury, Alzheimer's and Parkinson's diseases), and blocking cell cycle progression can prevent neuron death in some instances, endogenous cell cycle inhibition by p21 may be beneficial in such cases (Herrup and Yang, 2007; Majdzadeh et al., 2008; Stoica et al., 2009). Cytoplasmic p21 can protect cortical neurons from excitotoxicity and oxidative stress-induced apoptosis (Harms et al., 2007), and promote axonal regeneration following spinal cord injury by inhibiting RhoA, an effector of inhibitory molecules present in the central nervous system following injury (Tanaka et al., 2002; 2004). p21 expression is increased in tissue vulnerable to secondary degeneration following experimental stroke and peripheral axotomy, where it is suggested to

contribute to neuroprotection and spontaneous regeneration (Bonilla et al., 2002; Carmichael et al., 2005; van Lookeren Campagne and Gill, 1998).

Using a glutathione depletion model of oxidative stress, we observed that pharmacologically diverse chemicals that protect cortical neurons from glutathione depletion-mediated apoptosis also upregulate p21 transcription. This includes the anticancer drug mithramycin, histone deacetylase inhibitor trichostatin-A (TSA), and iron chelator desferrioxamine (DFO) (Langley et al., 2008; Sleiman et al., 2011; Zaman et al., 1999). With these agents, a cassette of protective genes is activated, with p21 contributing to the protective phenotype. Moreover, as aberrant cell cycle reentry is not evident following glutathione depletion in post mitotic neurons, the cell cycle-independent effectors of p21 appear to be important targets for neuroprotection. In this model, p21 overexpression is sufficient, but unnecessary for neuroprotection by TSA (Langley et al., 2008). These observations suggest that while unnecessary, p21 may be an efficient biomarker for neuroprotectants. Accordingly, targeting the transcriptional upregulation of p21 in neurons may be an ideal strategy to identify neuroprotective agents that avoid the potential toxicity of fostering overt tumor growth.

Materials and Methods

Protocols involving animals were approved by the Burke/Weill-Cornell IACUC and conform to the NIH guidelines for the use and care of laboratory animals. Wild type timed-pregnant mice (CD-1 strain, Charles River, Wilmington, MA) were used for the initial neuroprotection screens, and subsequently with the HIF-PHD inhibitor experiments. Concentration-response curves for the candidate p21 activators were generated using p21-null (B6;129S2-Cdkn1a^{tm1Tyj}/J, Jackson Laboratory, Bar Harbor, ME) and wild type animals of the same genetic background (B612SF2/J, Jackson Laboratory) to assess p21 necessity (Brugarolas et al., 1995).

Small molecule library and drug compounds

The Microsource Spectrum Collection (Microsource Discovery Systems, Gaylordsville, CT) was used for our high content screening and initial verification of neuroprotection. This is a library of FDA-approved drugs and natural product/bioactive small molecules. The detailed characterization of the candidate p21-inducers and HIF-PHD inhibitors was carried out using purified compounds obtained from Sigma (St. Louis, MO).

p21 promoter-reporter assay

Murine HT22 hippocampal neuronal cells (a gift from D. Schubert, Salk Institute, La Jolla, CA) stably transfected with a firefly luciferase reporter driven by 2.4 kb (el-Deiry et al., 1993) or 60 bp (Xiao et al., 1999) of the p21 proximal promoter were plated in 96-well plates in DMEM + 10% FBS for 24 hours. Compounds were added at a final concentration of 10 μM from 1000x DMSO stocks (Microsource). After 24 hours, luciferase activity was measured (Promega, Madison, WI) in a LMaxII luminometer (Molecular Devices, Sunnyvale, CA). Luminescence readings were normalized to cell survival of identically-treated sister cultures assessed by MTT reduction (Promega).

Neuron drug treatments and survival assays

Mouse cortical neurons were isolated from WT or p21-null E14.5 embryos as previously described (Zaman et al., 1999) and plated in MEM + 10% FBS + 5% horse serum (HS) + penicillin/streptomycin. The cultures were grown for 1 day to allow neurons to attach and extend neurites. Neurons were then co-treated with p21 inducers and homocysteic acid (HCA, 5 mM), a glutamate analog that prevents cystine uptake by the Xc^- antiporter. This causes neuronal apoptosis by glutathione depletion that is independent of glutamate receptor activation (Ratan et al., 2002). Viability was assessed 24 hours later by MTT reduction, and confirmed using a live-dead assay (Invitrogen, Carlsbad, CA) containing calcein-AM, which is retained in live cells, and ethidium homodimer, which accumulates in the nuclei of dead cells. Fluorescence micrographs were taken with a Zeiss Axiovert 200 microscope.

Cancer cell line assays

Murine Neuro-2A (N2A) neuroblastoma and human DLD-1 colon carcinoma cells (ATCC; Manassas, VA) were maintained in DMEM or RPMI 1640 + 10% FBS, and plated at 5,000 or 10,000 cells/well in 96-well plates (6.5 mm well diameter; Corning Costar, Tewsbury, MA), respectively. Drug treatments were added one hour later, following cell attachment to assess whether the compounds could alter the rate of cell proliferation. Phase contrast micrographs were acquired and cell viability was measured by MTT reduction after 24 hours. DLD-1 cells treated with HIF-PHD inhibitors were plated at 50,000 cells/well in 24-well plates (15.6 mm well diameter; Corning Costar) and viability was assessed 72 hours after treatment. For time course experiments with HIF-PHD inhibitors, viable N2A cells were loaded with calcein-AM at the indicated times. Whole-well fluorescence micrographs were taken with a Flash Cytometer (Trophos, Marseille, France) and cell counts made using MetaMorph (Molecular Devices).

HIF-PHD inhibitor cytotoxicity was tested on a panel of human neuroblastoma cell lines: NGP (gift of C.P. Reynolds), SH-SY5Y (ATCC), SK-N-SH, CHLA-15, and CHP-212 (Children's Oncology Cell Bank). Cell survival was determined in 96-well plates with the Digital Imaging Microscopy System (DIMSCAN), which uses fluorescence microscopy to quantify viable cells stained with fluorescein diacetate (FDA). The total fluorescence intensity per well after background quenching by eosin Y is proportional to cell viability (Frgala et al., 2007). 5,000-10,000 cells/well were plated and grown overnight before HIF-PHD inhibitors were added for 96 hours. FDA (10 μg/ml) and eosin Y (0.1%) were then added for 20 minutes. Total fluorescence per well was measured, and results expressed as the fluorescence ratio of treated to untreated wells.

The time points when cell viability was measured were determined empirically to highlight differences between drug treatments and control, and differed based on cancer cell type, culturing conditions, and viability assay.

Realtime RT-PCR

p21 gene expression was assessed by real time RT-PCR using TaqMan chemistry in a ABI Fast 7500 real time PCR system (Applied Biosystems, Carlsbad, CA) from cDNA libraries generated from RNA purified with Trizol (Invitrogen). Cortical neurons were treated for 8

hours prior to RNA harvest and assayed with a p21 probe (Cdkn1a; Mm01303209_m1) and β-actin as a housekeeping transcript. In N2A cells, RNA levels were assayed directly using a TaqMan One-step RNA-to-Ct Kit.

NGF deprivation of PC12 cells

PC12 cells were cultured on collagen-coated dishes with RPMI 1640 medium + 10% HS and 5% FBS as described previously, and differentiated with NGF (100 ηg/ml) in RPMI 1640 supplemented with 1% HS for 10-14 days (Farinelli and Greene, 1996). After differentiation, cells were deprived of NGF by washing basal media three times and maintaining cells in serum-free RPMI 1640 with anti-NGF antibody (1:100).

Western blot

Neurons were treated with the indicated compounds for 24 hours, after which neuronal proteins were harvested in NP40 lysis buffer (Tris-HCl 50 mM, NaCl 150 mM, EDTA 5 mM, NP-40 1%, pH 8.0; Boston Bioproducts, Worcester, MA) + 1x protease inhibitor cocktail (Sigma) + 1 mM PMSF (Sigma), assayed for protein content with the DC protein assay using a BSA standard (BioRad, Hercules, CA), and denatured in 1x NuPAGE LDS sample buffer (Tris-HCl 26.5 mM, Tris-base 35.3 mM, 0.5% LDS, 2.5% glycerol, 0.13 mM EDTA, 0.055 mM SERVA Blue G25, 0.044 mM phenol red, 50 mM DTT, ph 8.5; Invitrogen). 25 μg of protein were resolved through a 4-12% polyacrylamide gradient gel (Invitrogen) and then transferred onto nitrocellulose. Membranes were blocked for 1 hour in Odyssey blocking buffer (proprietary; LiCor, Lincoln NE), incubated overnight at 4°C with antibodies against p21 (1:250; mouse; clone OP76, Calbiochem, Darmstadt, Germany) and β-actin (1:5000; rabbit; Sigma), followed by fluorescent secondary antibodies (goat anti-mouse-IRDye800 and goat anti-rabbit-IRDye680; 1:20,000; LiCor) for 2 hours, and scanned using the LiCor infrared imaging system.

Retroviral transduction

Retroviruses delivering short-hairpin RNAs (shRNA) were generated as previously described (Aminova et al., 2005). The target sequences against HIF-1α and GFP plus a puromycin resistance gene were cloned into pSuperRetro vectors (OligoEngine) driven by the polymerase-III-H1-RNA gene promoter. N2A cells were transduced with the retroviruses for 1 hour at 37°C at a multiplicity of infection of 10 in the presence of 4 μg/ml polybrene, a cationic polymer that enhances retroviral transduction efficiency. The virus was then removed and cells were incubated for 24 hours in complete media prior to maintenance in puromycin (4 μg/ml, Sigma) to select for stable transductants.

Neurite outgrowth analysis

Neurite outgrowth and cell counts were assessed from fluorescence micrographs of calcein-labeled cortical neurons treated with HIF-PHD inhibitors using the Neurite Outgrowth application in Metamorph (Molecular Devices). Cell counts are expressed as the mean of neurons per microscope field using 10-12 fields per condition from 3 independent neuron preparations. Neurite branching and total outgrowth per neuron were expressed as the mean parameter per neuron from the same images.

Computer modeling

Docking experiments were performed using the CDOCKER algorithm as implemented Discovery Studio 2.5 (Accelrys, San Diego, CA), followed by force field minimization and binding energy calculations using the PHD2 crystal structure with the bound inhibitor (2G19.pdb) as the starting template. Preparation of the receptor was done by running a protein check and identifying all the elements of the structure. Force field minimization was carried out using the molecular mechanics algorithm CHARMm.

Statistical Analysis

All data are expressed as mean ± SEM and are plotted using GraphPad Prism. The statistical tests used are indicated in the figure legends. All results were repeated in at least 3 independent experiments. Statistical significance was taken at $P < 0.05$.

Results

We screened for transcriptional inducers of p21 using two promoter-reporter constructs containing either 60 bp or 2.4 kb of the p21 proximal promoter (Fig. 1a). The 2.4 kb reporter contains p53 binding sites that are activated by DNA damage, and thus activators of this reporter and not the 60 bp reporter may be undesirable (el-Deiry et al., 1993; Gartel and Radhakrishnan, 2005). We verified that HT22 cells stably expressing either construct cells could be activated by TSA, which is known to act through Sp1 sites in the 60 bp construct (Fig. 1a) (Langley et al., 2008), and that TSA also induced p21 mRNA and protein levels, confirming that our reporters faithfully mirrored endogenous gene expression (not shown).

Both reporter lines were screened against a small molecule library containing 2,000 FDA-approved drugs, natural products, and biologically active compounds (MicroSource Spectrum library). The results from both reporters were virtually identical, indicating that the initial 60 bp were sufficient for p21 transactivation by our hits, and that p21 induction is unlikely to be downstream of a DNA damage response (not shown). 93 compounds increased reporter activity by 2 standard deviations above the mean (Fig. 1b). These were screened in primary cortical neurons for p21 mRNA expression, basal toxicity, and neuroprotection from glutathione depletion at the screening concentration of 10 μM. Because some compounds showed basal toxicity, we also assessed neuroprotection with each compound at 1 μM (table S1). Of the neuroprotective compounds, we further characterized lycorine, chloroquine, 1,3-diphenylurea (DPU), N-acetylcysteine (NAC), and ciclopirox (CPO) because they conferred nearly complete neuroprotection from oxidative stress induced apoptosis.

Using purified compounds obtained from Sigma, we generated concentration-survival curves for each in the presence or absence of HCA (5 mM), a glutamate analogue that causes oxidative stress-induced cell death in immature cortical neurons. Extracellular HCA competitively inhibits cystine uptake, which depletes the intracellular antioxidant glutathione by depleting its rate-limiting precursor cysteine (Ratan et al., 2002). Each compound protected neurons from glutathione depletion: DPU, NAC, and TSA showed dose-dependent protection, while lycorine, chloroquine, and CPO were highly protective at

lower doses but exhibited basal toxicity at higher concentrations as assessed MTT reduction (Fig. 2a-2f). These results and the preservation of neuronal morphology were confirmed with live-dead labeling (Fig. S1). The protective concentrations varied for some compounds (i.e., chloroquine) compared to the initial screen, which may be due to differences in purity or stability of the compounds obtained from the Microsource library and Sigma.

To determine their effect on tumor cell growth, we tested each compound at the concentrations used for neuroprotection on human DLD-1 colorectal adenocarcinoma and murine N2A neuroblastoma cells, two established cancer cell lines. None of the hits increased the rate of cancer cell growth, while lycorine, CPO, and TSA significantly decreased cell number of both cell types over 24 h (Fig. 3a-f). Lycorine caused both cell types to assume spherical morphologies (Fig. 3a, S2b, S2h). Chloroquine did not change MTT reduction rates, but caused vacuole formation in DLD-1 cells (Fig. 3b, S2c, S2i). DPU had no effect on DLD-1 cells but prevented N2A cell proliferation (Fig. 3c, S2d, S2j). NAC, while protective to neurons, did not alter the growth rate or morphology (Fig. 3d, S2e, S2k). CPO treatment yielded fewer (Fig. 3e), and larger DLD-1 cells, and caused cytosolic vacuolization of both cell types (Fig. S2f and S2l). These anti-tumor effects correlated with p21 mRNA induction, as each compound, except NAC, which failed to inhibit tumor cell growth, induced p21 expression in N2A cells (Fig. S3a). Interestingly, despite upregulating p21 levels, chloroquine did not decrease viability at 24 hours, suggesting that other properties of these compounds may synergize with p21 induction to prevent the proliferation of DLD-1 and N2A cells. These data show that most of our lead hits upregulate p21 expression and inhibit proliferation in these cancer cell lines.

Of the neuroprotective and anti-tumor p21 inducers, only CPO killed both cancer cell types at concentrations that protected post-mitotic neurons without causing steady-state toxicity (1 μM, Fig. 2e and 3e). CPO is an iron chelator and canonical inhibitor of HIF-PHDs (Linden et al., 2003), which are oxygen, 2-oxoglutarate, and iron-dependent enzymes that hydroxylate HIFα isforms under normoxia, targeting them for proteasomal degradation (Epstein et al., 2001). Accordingly, we formulated a model whereby global pharmacological HIF-PHD inhibition (inhibition of all three PHD isoforms) leads to both neuroprotection and cessation of tumor growth. We tested whether other established, but structurally diverse HIF-PHD inhibitors (DFO 50 μM, an iron chelator, and DHB 20 μM and DMOG 250 μM, competitive inhibitors of 2-oxoglutarate) were also toxic to tumor cells. We treated DLD-1 cells with each drug for 72 h and found that they significantly decreased cell proliferation (Fig. 4f) and that CPO and DFO caused the formation of large and ubiquitous cytosolic vacuoles (Fig. 4b-c). All four compounds yielded larger, and thus fewer cells as compared to controls (Fig. 4a-e). Vacuole formation and large cells are reminiscent of a senescence phenotype, which is an important tumor suppression mechanism in some instances, and can be induced by forced expression of p21 (Rodier and Campisi, 2011). To further characterize the anti-tumor potential of HIF-PHD inhibitors, we tested them for cytotoxicity against a panel of five human neuroblastoma cell lines. Each compound showed significant cytotoxicity at concentrations similar those used with the N2A and DLD-1 cells (Table 1, Fig. S4).

Our previous studies showed that the neuroprotective effects of HIF-PHD inhibitors in hippocampal neuroblasts are independent of HIF-1α (Siddiq et al., 2009). To determine whether the anti-proliferative effects of these compounds required HIF-1α, we transduced N2A cells with retroviruses expressing shRNA against HIF-1α, which reduced HIF-1α mRNA levels to 30% of those expressing shGFP (Fig. S5a). When seeded at low density, siHIF-1α (not shown), siGFP (not shown), and untransduced cells (Fig. 5a.) formed nearly confluent patches by the third day in vitro. By contrast, when treated with HIF-PHD inhibitors, their proliferation rate was significantly inhibited (Fig. 5a-b, S5b). This toxicity was HIF-1α independent, as N2A cell proliferation was equally impaired by HIF-PHD inhibition when HIF-1α was knocked-down (Fig. S5b). Two independent HIFα isoforms, HIF-1α and HIF-2α, can activate the HIF pathway. We evaluated whether HIF-2α contributed to the effect of the HIF-PHD inhibitors, but unexpectedly, could not detect HIF-2α expression in the siGFP- or siHIF-1α-N2A cells (not shown).

Because p21 overexpression is sufficient to protect hippocampal neuroblasts or primary cortical neurons from glutathione depletion or peroxide insult (Langley et al., 2008), our initial model predicted that p21 protein induction would be necessary for neuroprotection. Nevertheless, p21 was dispensable for neuroprotection as our hits showed identical concentration-responses in neurons from mice with homozygous deletion of p21 (Fig. S6). Additionally, while all compounds induced p21 message at the screening dose (Fig. 1c), the lowest protective doses of lycorine (0.5 μM), chloroquine (0.5 μM), DPU (50 μM), and NAC (20 μM) did not stably induce p21 protein levels (Fig. S3b). Notably, only CPO induced p21 protein levels (Fig. S3b and 6b) at concentrations that were both basally nontoxic to neurons and inhibitory to cancer cell growth (Fig. 2e and 3e). We checked whether DFO, DHB, and DMOG also induced p21 mRNA and protein levels in neurons, and as expected, each induced p21 mRNA (Fig. 6a), while all but DMOG also increased p21 protein levels (Fig. 6b). At these concentrations, all but DMOG showed complete protection from HCA (Fig. 6c), suggesting that induction of p21 protein may be a good marker of neuroprotection by HIF-PHD inhibitors. As the anti-tumor effect of these compounds progressed over 3 days, we assessed whether they would be toxic to primary neurons over the same time course. Calcein labeling of neurons treated for 3 days with HIF-PHD inhibitors showed no decrease in cell number compared to controls (Figs. 6d-h and table S2). Interestingly, neurons treated with DFO, CPO, and DHB exhibited increased neurite branching compared to untreated cells, whereas DMOG impaired these aspects of neurite outgrowth (Fig. 6d-f and table S2).

DFO and CPO have been reported to protect sympathetic neurons and differentiated PC12 cells from NGF deprivation by preventing aberrant cell cycle reentry and subsequent apoptosis (Ferrari and Greene, 1994). To see whether this correlated with p21 protein induction, p21 protein levels were assessed in differentiated PC12 cells treated with CPO for 6.5 hours. Indeed, treatment with CPO (4 μM) significantly induced p21 protein levels (Fig. S7).

DFO is a large molecule (MW 656.79) that likely inhibits HIF-PHDs by chelating extracellular Fe^{2+}, thereby limiting the intracellular Fe^{2+} required for catalysis (Zaman et al., 1999). In contrast, CPO, DHB, and DMOG are of lower molecular weight (all <268.35 MW), and could directly inhibit HIF-PHDs intracellularly by binding within their conserved

catalytic domain. To assess this, we docked each molecule within a model of the PHD2 catalytic site derived from a crystal structure (2g19.pdb) (McDonough et al., 2006) using the CDOCKER algorithm. Each compound fit within the binding pocket of PHD2 and coordinated the catalytic Fe^{2+} in the least energy conformations (Fig. S3c-e).

Discussion

Chronically inhibiting the pathways that contribute to neuron death has been shown in some cases to promote tumor growth. This is exemplified by p53 or targeted PTEN deletion in mice where neuron death is abrogated (Crumrine et al., 1994; Domanskyi et al., 2011; Liu et al., 2010; Park et al., 2008), but the risk for developing tumors increases (Donehower et al., 1992; Hollander et al., 2011). By targeting p21, an effector that is simultaneously neuroprotective and anti-tumor, we overcome this potential problem. Indeed, we identified diverse neuroprotective and anti-tumor p21 inducers, including HIF-PHD inhibitors. Each structurally diverse HIF-PHD inhibitor killed nearly all cancer cell lines tested at concentrations that protected post-mitotic neurons without causing steady-state toxicity. This result was initially surprising as HIF-PHDs are important negative regulators of the HIF pathway, and HIF activation upregulates the transcription of genes involved in glycolysis, pH regulation, angiogenesis, cell proliferation, and survival pathways, all of which are known to promote tumor growth (Semenza, 2010).

While HIF has been widely regarded as oncogenic, the role of HIF in tumorigenesis is complex as it may also repress tumor growth depending on cell type and tissue context (Blancher et al., 2000; Carmeliet et al., 1998). For instance, tumor-causing IDH1 mutations (R123H) increase PHD2 activity, which diminishes HIF levels, but enhances tumor cell proliferation. Conversely, PHD2 knockdown and subsequent HIF activation in transformed astrocytes bearing IDH mutations inhibited colony formation on soft agar (Koivunen et al., 2012). In glioblastoma cells, HIF-PHD inhibition with DMOG or PHD2/PHD3 knockdown causes cell death and sensitization to hypoxia by disrupting the feedback expression of PHD2/PHD3 that serves to maintain the proper levels of HIF activity. The overexpression of HIF-2α in glioblastoma xenografts increased angiogenesis, but reduced tumor size due to increased tumor cell apoptosis *in vivo* (Acker et al., 2005; Henze et al., 2010). Furthermore, there is evidence that HIF-PHD inhibition may not be equivalent to tumorigenic HIF activation, as hepatic Vhl deletion, which activates HIF, causes benign tumors, whereas combined deletion of all three HIF-PHD isoforms does not (Haase et al., 2001; Minamishima and Kaelin, 2010).

More recently, other targets for prolyl-hydroxylation have emerged that contribute to tumor growth by HIF-dependent and -independent mechanisms. One study reported that PHD3 mediates metabolic reprogramming of cancer cells through the prolyl-hydroxylation of pyruvate kinase-M2 (PKM2). Proline-hydroxylated PKM2 becomes a coactivator for the transactivation of HIF-1α target genes, including those that mediate glycolytic adaptation to hypoxia (Luo et al., 2011). In another study, PHD1 knockdown limited proliferation of estrogen-dependent breast cancer cells by a hydroxylase-dependent, but HIF-independent reduction of cyclin D1 expression, though the precise targets of PHD1 hydroxylation were not identified (Zhang et al., 2009).

The lack of necessity of HIF-1α expression for HIF-PHD inhibitor cytotoxicity in N2A cells suggest that other HIF-PHD targets, in addition to HIF may be important for this effect. In our studies, we have pharmacologically inhibited the activity of all HIF-PHD isoforms, which may engage multiple synergistic anti-tumor pathways (i.e. through PHD1/PHD3 inhibition and p21 induction), despite stabilizing HIF. Accordingly, our data suggest that global HIF-PHD inhibition in these cancer cell lines does not lead to increased cell proliferation, but rather, limits cell proliferation or causes cell death. We have previously reported that the neuroprotection by HIF-PHD inhibitors is also HIF-1α-independent and can be recapitulated by the individual knockdown of PHD1 (and not PHD2 or PHD3) (Siddiq et al., 2009), suggesting that neuronal degeneration and tumorigenesis may share common pathways. The precise neuroprotective and anti-tumor targets of the HIF-PHDs are currently being pursued in our labs. Importantly, these in vitro results set the table for assessing HIF-PHD inhibitors in animal models, which will provide the ultimate validation of their effect on basal tumor formation with chronic use.

Though our initial model predicted that p21 protein induction would be necessary for neuroprotection, we found that p21 was dispensable for neuroprotection in our oxidative stress model (Fig. S6). This was echoed by the observation that the protective doses of some hits did not stably induce p21 protein levels (Fig. S3b), suggesting that p21 protein upregulation was transient or that some agents may upregulate transcription, but not provide the translational drive to convert new p21 mRNA into protein. It is likely that functional redundancy of genes induced by these compounds precludes a large contribution by any single gene product, including p21. As such, this suggests that p21 induction serves as a good biomarker for the activation of neuroprotective transcriptional programs (Fig. 7).

Though p21 was unnecessary for neuroprotection from glutathione depletion, we anticipate that these agents will be protective in disease models where inappropriate activation of cell cycle components appears to drive neurodegeneration (Greene et al., 2007; Heintz, 1993; Herrup and Yang, 2007; Park et al., 2007; Vincent et al., 2003). Intriguingly, CPO and DFO have previously been shown to protect neuron-like differentiated PC12 cells from NGF deprivation, a model where aberrant activation of cell cycle components mediates cell death (Farinelli and Greene, 1996). We confirmed that CPO upregulates p21 in differentiated PC12 cells (Fig. S7), suggesting that CPO and DFO may inhibit aberrant reentry of post-mitotic neurons by inducing p21. Moreover DFO has been shown to protect the brain from many acute and chronic neurodegenerative conditions (Hanson et al., 2009; Zhao and Rempe, 2011).

Importantly, our data suggests that assessing the effect of potential neuroprotective agents on cancer cell growth warrants legitimate consideration. Given the parallels between neurodegeneration and oncogenesis, targets such as p21 that address pathological processes in both conditions may prove to be an efficient way to identify therapeutics that are safe for chronic use. Following this strategy, we have found that PHD inhibition and HIF activation does not necessarily lead to tumor formation or malignant transformation, which supports the mounting evidence for a pro-oncogenic role for PHDs in tumor cells. This also argues for the propitious use of PHD inhibitors not only for cancer therapy but also for the chronic treatment of neurological disease.

Supplementary Material

Refer to Web version on PubMed Central for supplementary material.

Acknowledgments

This work was supported by National Institutes of Health Grants NIA P01-AG014930 (Project 1) to R.R.R., and NCI R25-CA105012 to T.C.M., the New York State Spinal Cord Injury Research Board Center of Research Excellence Grant to R.R.R., the Miriam and Sheldon Adelson Program in Neurorehabilitation and Neural Repair to R.R.R., the Burke Foundation, and the Tay-Bandz Foundation to D.J.Y.

Abbreviations

CPO	ciclopirox
DFO	desferrioxamine
DHB	3,4-dihydroxybenzoate
DMOG	dimethyloxallyl glycine
HIF	hypoxia inducible factor
NGF	nerve growth factor
PHD	proyl-4-hydroxylase

References

Acker T, et al. Genetic evidence for a tumor suppressor role of HIF-2alpha. Cancer Cell. 2005; 8:131–41. [PubMed: 16098466]

Aminova LR, et al. Prosurvival and prodeath effects of hypoxia-inducible factor-1alpha stabilization in a murine hippocampal cell line. J Biol Chem. 2005; 280:3996–4003. [PubMed: 15557337]

Blancher C, et al. Relationship of hypoxia-inducible factor (HIF)-1alpha and HIF-2alpha expression to vascular endothelial growth factor induction and hypoxia survival in human breast cancer cell lines. Cancer Res. 2000; 60:7106–13. [PubMed: 11156418]

Bonilla IE, et al. Small proline-rich repeat protein 1A is expressed by axotomized neurons and promotes axonal outgrowth. J Neurosci. 2002; 22:1303–15. [PubMed: 11850458]

Brugarolas J, et al. Radiation-induced cell cycle arrest compromised by p21 deficiency. Nature. 1995; 377:552–7. [PubMed: 7566157]

Carmeliet P, et al. Role of HIF-1alpha in hypoxia-mediated apoptosis, cell proliferation and tumour angiogenesis. Nature. 1998; 394:485–90. [PubMed: 9697772]

Carmichael ST, et al. Growth-associated gene expression after stroke: evidence for a growth-promoting region in peri-infarct cortex. Exp Neurol. 2005; 193:291–311. [PubMed: 15869933]

Crumrine RC, et al. Attenuation of p53 expression protects against focal ischemic damage in transgenic mice. Journal of cerebral blood flow and metabolism : official journal of the International Society of Cerebral Blood Flow and Metabolism. 1994; 14:887–91. [PubMed: 7929653]

Domanskyi A, et al. Pten ablation in adult dopaminergic neurons is neuroprotective in Parkinson's disease models. The FASEB journal : official publication of the Federation of American Societies for Experimental Biology. 2011

Donehower LA, et al. Mice deficient for p53 are developmentally normal but susceptible to spontaneous tumours. Nature. 1992; 356:215–21. [PubMed: 1552940]

el-Deiry WS, et al. WAF1, a potential mediator of p53 tumor suppression. Cell. 1993; 75:817–25. [PubMed: 8242752]

Epstein AC, et al. C. elegans EGL-9 and mammalian homologs define a family of dioxygenases that regulate HIF by prolyl hydroxylation. Cell. 2001; 107:43–54. [PubMed: 11595184]

Farinelli SE, Greene LA. Cell cycle blockers mimosine, ciclopirox, and deferoxamine prevent the death of PC12 cells and postmitotic sympathetic neurons after removal of trophic support. J Neurosci. 1996; 16:1150–62. [PubMed: 8558244]

Ferrari G, Greene LA. Proliferative inhibition by dominant-negative Ras rescues naive and neuronally differentiated PC12 cells from apoptotic death. EMBO J. 1994; 13:5922–8. [PubMed: 7813431]

Frgala T, et al. A fluorescence microplate cytotoxicity assay with a 4-log dynamic range that identifies synergistic drug combinations. Mol Cancer Ther. 2007; 6:886–97. [PubMed: 17363483]

Gartel AL, Radhakrishnan SK. Lost in transcription: p21 repression, mechanisms, and consequences. Cancer Res. 2005; 65:3980–5. [PubMed: 15899785]

Gartel AL, Tyner AL. The role of the cyclin-dependent kinase inhibitor p21 in apoptosis. Mol Cancer Ther. 2002; 1:639–49. [PubMed: 12479224]

Greene LA, et al. Cell cycle molecules define a pathway required for neuron death in development and disease. Biochimica et biophysica acta. 2007; 1772:392–401. [PubMed: 17229557]

Haase VH, et al. Vascular tumors in livers with targeted inactivation of the von Hippel-Lindau tumor suppressor. Proc Natl Acad Sci U S A. 2001; 98:1583–8. [PubMed: 11171994]

Hanson LR, et al. Intranasal deferoxamine provides increased brain exposure and significant protection in rat ischemic stroke. The Journal of pharmacology and experimental therapeutics. 2009; 330:679–86. [PubMed: 19509317]

Harms C, et al. Phosphatidylinositol 3-Akt-kinase-dependent phosphorylation of p21(Waf1/Cip1) as a novel mechanism of neuroprotection by glucocorticoids. J Neurosci. 2007; 27:4562–71. [PubMed: 17460069]

Heintz N. Cell death and the cell cycle: a relationship between transformation and neurodegeneration? Trends Biochem Sci. 1993; 18:157–9. [PubMed: 8328013]

Henze AT, et al. Prolyl hydroxylases 2 and 3 act in gliomas as protective negative feedback regulators of hypoxia-inducible factors. Cancer Res. 2010; 70:357–66. [PubMed: 20028863]

Herrup K, Yang Y. Cell cycle regulation in the postmitotic neuron: oxymoron or new biology? Nat Rev Neurosci. 2007; 8:368–78. [PubMed: 17453017]

Hollander MC, et al. PTEN loss in the continuum of common cancers, rare syndromes and mouse models. Nature reviews. Cancer. 2011; 11:289–301.

Koivunen P, et al. Transformation by the (R)-enantiomer of 2-hydroxyglutarate linked to EGLN activation. Nature. 2012

Langley B, et al. Pulse inhibition of histone deacetylases induces complete resistance to oxidative death in cortical neurons without toxicity and reveals a role for cytoplasmic p21(waf1/cip1) in cell cycle-independent neuroprotection. J Neurosci. 2008; 28:163–76. [PubMed: 18171934]

Linden T, et al. The antimycotic ciclopirox olamine induces HIF-1alpha stability, VEGF expression, and angiogenesis. FASEB J. 2003; 17:761–3. [PubMed: 12594177]

Liu K, et al. PTEN deletion enhances the regenerative ability of adult corticospinal neurons. Nat Neurosci. 2010; 13:1075–81. [PubMed: 20694004]

Luo W, et al. Pyruvate Kinase M2 Is a PHD3-Stimulated Coactivator for Hypoxia-Inducible Factor 1. Cell. 2011; 145:732–44. [PubMed: 21620138]

Majdzadeh N, et al. Class IIA HDACs in the regulation of neurodegeneration. Front Biosci. 2008; 13:1072–82. [PubMed: 17981613]

McDonough MA, et al. Cellular oxygen sensing: Crystal structure of hypoxia-inducible factor prolyl hydroxylase (PHD2). Proceedings of the National Academy of Sciences of the United States of America. 2006; 103:9814–9. [PubMed: 16782814]

Minamishima YA, Kaelin WG Jr. Reactivation of hepatic EPO synthesis in mice after PHD loss. Science. 2010; 329:407. [PubMed: 20651146]

Park DS, et al. Cyclin dependent kinase inhibitors and dominant negative cyclin dependent kinase 4 and 6 promote survival of NGF-deprived sympathetic neurons. J Neurosci. 1997; 17:8975–83. [PubMed: 9364045]

Park KH, et al. Conditional neuronal simian virus 40 T antigen expression induces Alzheimer-like tau and amyloid pathology in mice. J Neurosci. 2007; 27:2969–78. [PubMed: 17360920]

Park KK, et al. Promoting axon regeneration in the adult CNS by modulation of the PTEN/mTOR pathway. Science. 2008; 322:963–6. [PubMed: 18988856]

Ratan RR, et al. In vitro model of oxidative stress in cortical neurons. Methods in enzymology. 2002; 352:183–90. [PubMed: 12125346]

Rodier F, Campisi J. Four faces of cellular senescence. The Journal of cell biology. 2011; 192:547–56. [PubMed: 21321098]

Semenza GL. Defining the role of hypoxia-inducible factor 1 in cancer biology and therapeutics. Oncogene. 2010; 29:625–34. [PubMed: 19946328]

Siddiq A, et al. Selective inhibition of hypoxia-inducible factor (HIF) prolyl-hydroxylase 1 mediates neuroprotection against normoxic oxidative death via HIF- and CREB-independent pathways. J Neurosci. 2009; 29:8828–38. [PubMed: 19587290]

Sleiman SF, et al. Mithramycin is a gene-selective Sp1 inhibitor that identifies a biological intersection between cancer and neurodegeneration. J Neurosci. 2011; 31:6858–70. [PubMed: 21543616]

Stoica BA, et al. Cell cycle activation and CNS injury. Neurotox Res. 2009; 16:221–37. [PubMed: 19526282]

Tanaka H, et al. Cytoplasmic p21(Cip1/WAF1) regulates neurite remodeling by inhibiting Rhokinase activity. J Cell Biol. 2002; 158:321–9. [PubMed: 12119358]

Tanaka H, et al. Cytoplasmic p21(Cip1/WAF1) enhances axonal regeneration and functional recovery after spinal cord injury in rats. Neuroscience. 2004; 127:155–64. [PubMed: 15219678]

van Lookeren Campagne M, Gill R. Increased expression of cyclin G1 and p21WAF1/CIP1 in neurons following transient forebrain ischemia: comparison with early DNA damage. J Neurosci Res. 1998; 53:279–96. [PubMed: 9698156]

Vincent I, et al. The cell cycle and human neurodegenerative disease. Progress in cell cycle research. 2003; 5:31–41. [PubMed: 14593698]

Xiao H, et al. Both Sp1 and Sp3 are responsible for p21waf1 promoter activity induced by histone deacetylase inhibitor in NIH3T3 cells. J Cell Biochem. 1999; 73:291–302. [PubMed: 10321829]

Zaman K, et al. Protection from oxidative stress-induced apoptosis in cortical neuronal cultures by iron chelators is associated with enhanced DNA binding of hypoxia-inducible factor-1 and ATF-1/CREB and increased expression of glycolytic enzymes, p21(waf1/cip1), and erythropoietin. J Neurosci. 1999; 19:9821–30. [PubMed: 10559391]

Zhang Q, et al. Control of cyclin D1 and breast tumorigenesis by the EglN2 prolyl hydroxylase. Cancer cell. 2009; 16:413–24. [PubMed: 19878873]

Zhao Y, Rempe DA. Prophylactic neuroprotection against stroke: low-dose, prolonged treatment with deferoxamine or deferasirox establishes prolonged neuroprotection independent of HIF-1 function. Journal of cerebral blood flow and metabolism : official journal of the International Society of Cerebral Blood Flow and Metabolism. 2011; 31:1412–23. [PubMed: 21245873]

Highlights

- Targets for chronic neuroprotection should not promote cancer/tumor formation
- We screened for transcriptional inducers of $p21^{waf1/cip1}$ (p21), a CDK inhibitor
- p21 inducers protect neurons from cell death and prevent cancer cell proliferation
- HIF-PHD inhibitors induce $p21^{waf1/cip1}$ and are both neuroprotective and antitumor
- HIF-PHD inhibitors should not promote tumor formation despite stabilizing HIF

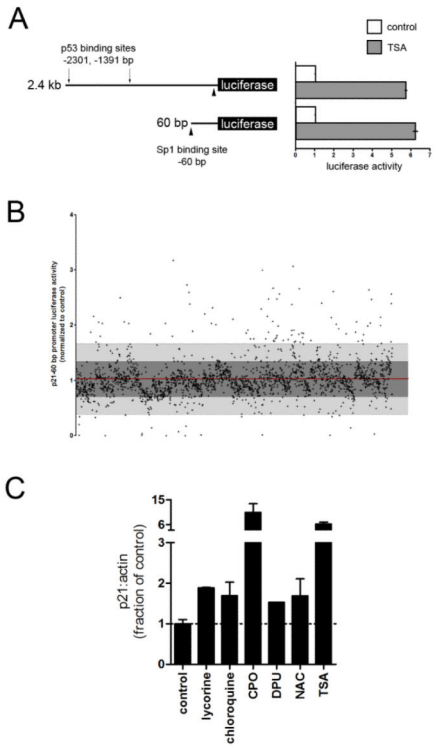

Figure 1.

Biological screen for transcriptional inducers of p21. ***A***, HT22 cells were stably transfected with a firefly luciferase reporter driven by 2.4 kb or 60 bp of the p21 proximal promoter. The 2.4 kb reporter contains the p53 binding sites (arrows) necessary for activation by DNA damage. Both constructs are responsive to TSA, which activates the Sp1 sites (arrow heads). ***B***, A 2,000 compound library of FDA-approved drugs and natural product small molecules were screened using the 60 bp promoter. Compounds that induced reporter activity by ≥ 2 SD (above light grey region) were further investigated. ***C***, p21 mRNA levels from primary cortical neurons treated with neuroprotective hits (10 μM). TSA was included as a positive control.

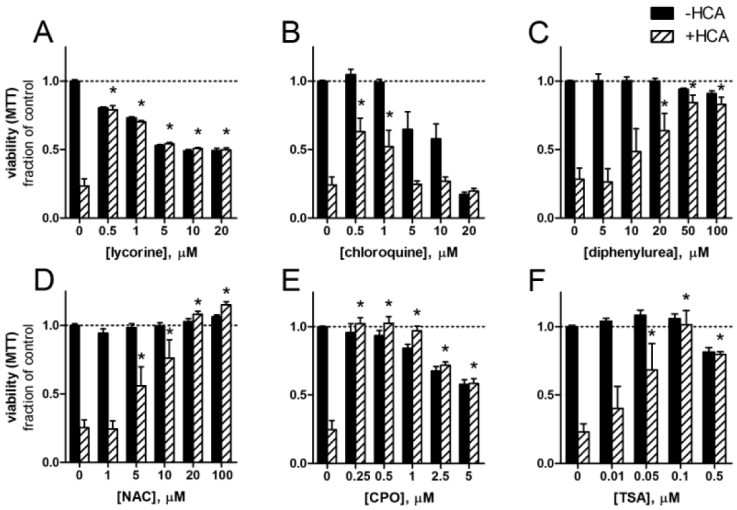

Figure 2.

p21 inducers are neuroprotective against oxidative stress-induced neuron death. ***A-F***, E14.5 mouse cortical neurons were treated with the p21 inducers alone (closed bars) or with HCA (5 mM, open bars), which inhibits cystine uptake causing the depletion of intraneuronal glutathione. This causes neuron death which was assessed by MTT reduction after 24 h. Viability of HCA-treated neurons in the absence of neuroprotective compounds was significantly less than controls, *P<0.001*, *=*P<0.01* vs. +HCA only, two-way ANOVA-Bonferroni's *post* test, n=6.

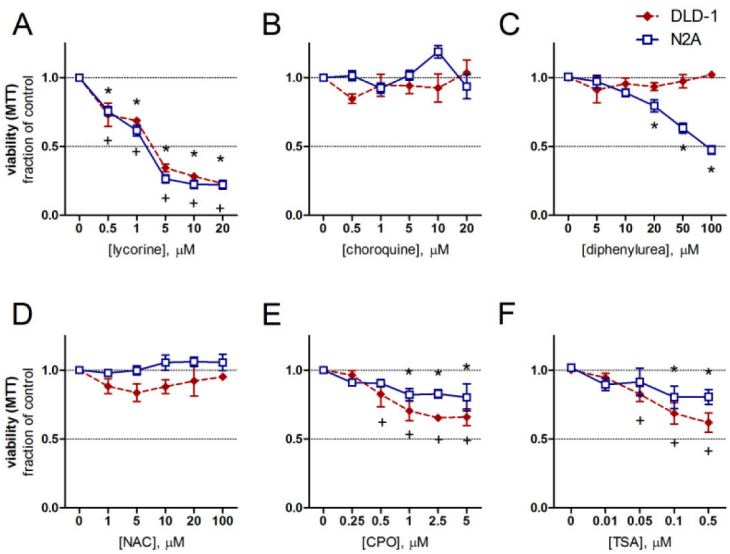

Figure 3.

p21 inducers limit the proliferation of DLD-1 adenocarcinoma and N2A neuroblastoma cells. ***A-F***, DLD-1 (*red diamonds*) and N2A (*blue squares*) were treated with the indicated compounds immediately after attachment and assayed for viability by MTT reduction 24 h later. +=*P<0.05* vs. DLD-1 control, *=*P<0.05* vs. N2A control, two-way ANOVA-Bonferroni's *post* test, n=3.

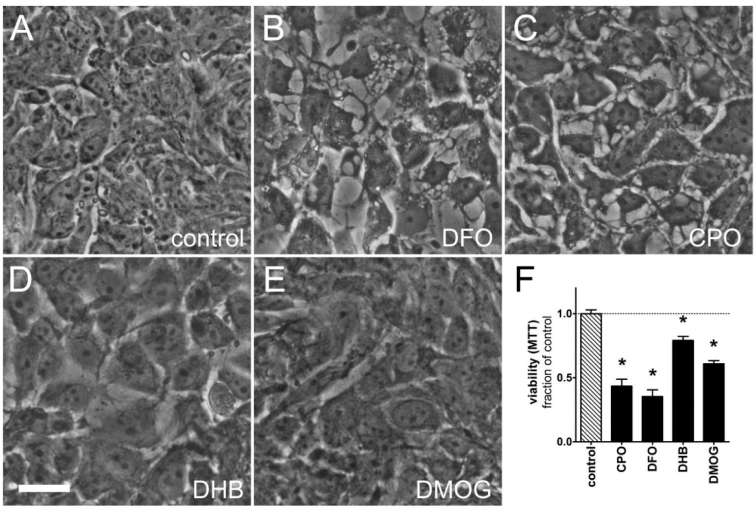

Figure 4.

HIF-PHD inhibitors decrease the viability of DLD-1 cells. ***A***-***E***, phase contrast images of ***A***, untreated DLD-1 cells or cells treated with ***B***, DFO 50 μM, ***C***, CPO 1 μM, ***D***, DHB 20 μM, or ***E***, DMOG 250 μM for 72 h. CPO or DFO (***B*** *and* ***C***) caused the formation of large cytosolic vacuoles, while all compounds yielded larger cells. ***F***, DLD-1 cultures were assayed for viability by MTT reduction following treatment with HIF-PHD inhibitors. Scale bar = 25 μm. *=$P<0.01$ vs. control, one-way ANOVA-Bonferroni's *post* test, n=8.

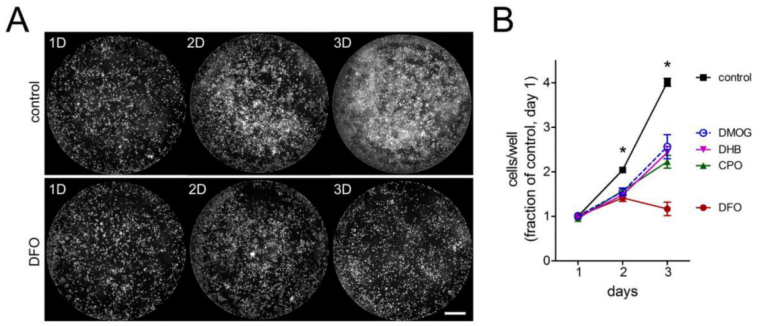

Figure 5.

HIF-PHD inhibitors prevent N2A cell proliferation. ***A-B***, N2A cells were plated in 96-well plates, treated with HIF-PHD inhibitors, and then assayed for viability by calcein labeling and cell counting with a flash cytometer. ***A***, N2A cells proliferate over 3 days (top) to cover the well surface, whereas proliferation is inhibited in DFO-treated cells (bottom). ***B***, cell counts from cultures treated with DFO 50 μM, CPO 1 μM, DHB 20 μM, or DMOG 250 μM show that HIF-PHD inhibition impeded N2A cell proliferation compared untreated cells. Scale bar = 1 mm. Data are normalized to cell counts from control wells on day 1. Cell counts from PHD inhibitor-treated cells are significantly lower than control at days 2 and 3, *=$P<0.01$, two-way ANOVA-Bonferroni's *post* test, n=8.

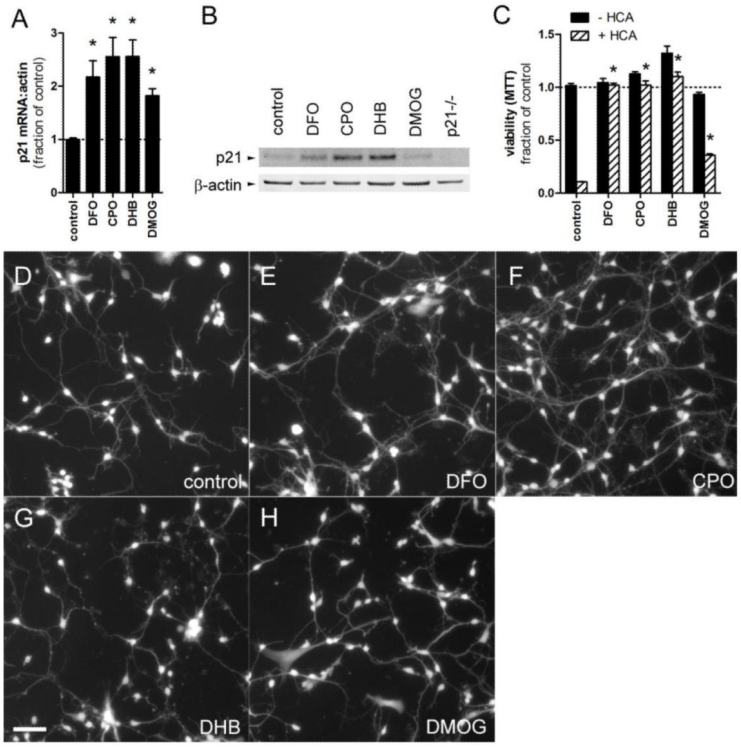

Figure 6.

HIF-PHD inhibitors upregulate p21 and protect cortical neurons from glutathione depletion-mediated cell death. ***A-H***, E14.5 mouse cortical neurons were treated with the concentrations of HIF-PHD inhibitors that were toxic to DLD-1 and N2A in figures 4 and 5: DFO 50 μM, CPO 1 μM, DHB 20 μM, and DMOG 250 μM. ***A***, each compound upregulated p21 mRNA levels, *=*P<0.05*, one-way ANOVA-Bonferroni's post test, n=7, ***B***, while all but DMOG upregulated p21 protein levels. ***C***, oxidative stress was induced by glutathione depletion with HCA 5 mM. Co-treatment with DFO, CPO, and DHB completely protected neurons from cell death. *=P<0.001, two-way ANOVA-Bonferroni's post test, n=4. ***D-H***, fluorescence micrographs of calcein-labeled cortical neurons treated for 3 days with HIF-PHD inhibitors show no basal toxicity. Note the more robust neurite outgrowth in DFO and CPO-treated neurons compared to controls (***D-F***). Scale bar = 25 μm.

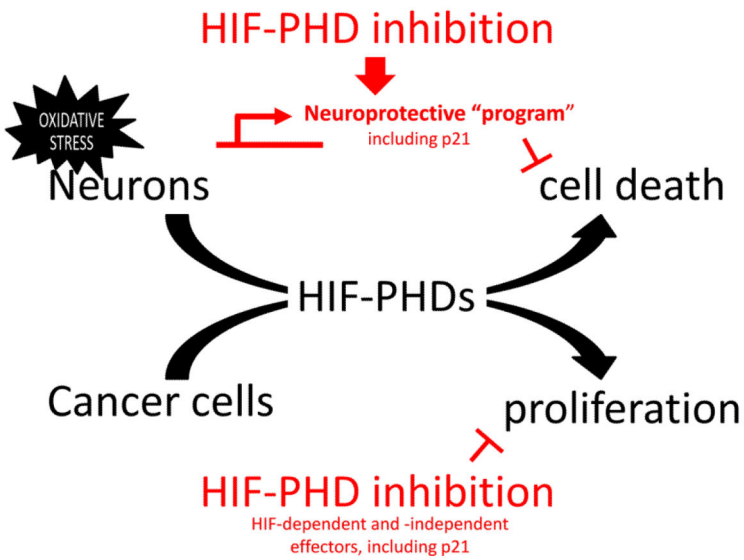

Figure 7.

Working model of HIF-PHD-mediated neuroprotection and suppression of cancer cell proliferation. HIF-PHD inhibition and the other identified p21 inducers activate the transcription of a broad neuroprotective program that prevents oxidative stress-induced neuronal apoptosis. The breadth of this program precludes the necessity of any single member of the program (i.e. p21 is sufficient to protect, but is unnecessary for the neuroprotective actions of these compounds). Likewise, HIF-PHD inhibitors can induce HIF-dependent cell death, or interfere with PHD-dependent, but HIF-independent survival pathways in cancer cells. It is formally possible that the HIF-PHD targets that mediate neuron death following oxidative stress are the same as those driving tumorigenesis.

Table 1

IC^{50} values (μM) of canonical HIF-PHD inhibitors for human neuroblastoma cell lines.

	CHLA15	SH-SY5Y	SK-N-SH	CHP212	NGP
CPO	0.42	0.41	0.68	0.53	0.61
DFO	1.14	0.78	3.56	N.D.	1.59
DHB	4.1	8.3	30.7	25.4	4.5
DMOG	18.3	957.5	557.8	223.5	497.9